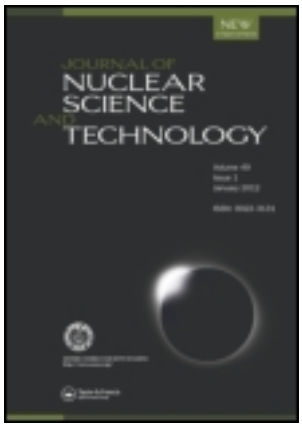

Journal of Nuclear Science and Technology
Publication details, including instructions for authors and subscription information:
http://www.tandfonline.com/loi/tnst20

Reactivity Coefficients in BN-600 Core with Minor Actinides

Andrei RINEISKI [a], Makoto ISHIKAWA [b], Jinwook JANG [c], Prabhakaran MOHANAKRISHNAN [d], Tim NEWTON [e], Gérald RIMPAULT [f], Alexander STANCULESCU [g] & Victor STOGOV [h]

[a] Karlsruhe Institute of Technology (KIT), B. 421, 76344, Eggenstein-Leopoldshafen, Germany

[b] Japan Atomic Energy Agency (JAEA), Ibaraki, 311-1393, Japan

[c] Korea Atomic Energy Research Institute (KAERI), Yusong, Taejon, 305-600, Korea

[d] Indira Gandhi Centre for Atomic Research (IGCAR), Kalpakkam, Tamil Nadu, 603 102, India

[e] SERCO, Winfrith, Dorchester, Dorset, DT2 8DH, United Kingdom

[f] CEA Cadarache Centre, F-13108, Saint-Paul-lez-Durance Cedex, France

[g] International Atomic Energy Agency (IAEA), Wagramer Strasse 5, A-1400, Vienna, Austria

[h] Institute for Physics and Power Engineering (IPPE), Bondarenko Sq. 1, 249033, Obninsk, Russia

Published online: 05 Jan 2012.

To cite this article: Andrei RINEISKI, Makoto ISHIKAWA, Jinwook JANG, Prabhakaran MOHANAKRISHNAN, Tim NEWTON, Gérald RIMPAULT, Alexander STANCULESCU & Victor STOGOV (2011) Reactivity Coefficients in BN-600 Core with Minor Actinides, Journal of Nuclear Science and Technology, 48:4, 635-645

To link to this article: http://dx.doi.org/10.1080/18811248.2011.9711744

Journal of NUCLEAR SCIENCE and TECHNOLOGY, Vol. 48, No. 4, p. 635–645 (2011)

ARTICLE

Reactivity Coefficients in BN-600 Core with Minor Actinides

Andrei RINEISKI[1,*], Makoto ISHIKAWA[2], Jinwook JANG[3], Prabhakaran MOHANAKRISHNAN[4], Tim NEWTON[5], Gérald RIMPAULT[6], Alexander STANCULESCU[7] and Victor STOGOV[8]

[1]*Karlsruhe Institute of Technology (KIT), B. 421, 76344 Eggenstein-Leopoldshafen, Germany*
[2]*Japan Atomic Energy Agency (JAEA), Ibaraki 311-1393, Japan*
[3]*Korea Atomic Energy Research Institute (KAERI), Yusong, Taejon 305-600, Korea*
[4]*Indira Gandhi Centre for Atomic Research (IGCAR), Kalpakkam Tamil Nadu 603 102, India*
[5]*SERCO, Winfrith, Dorchester, Dorset, DT2 8DH, United Kingdom*
[6]*CEA Cadarache Centre, F-13108 Saint-Paul-lez-Durance Cedex, France*
[7]*International Atomic Energy Agency (IAEA), Wagramer Strasse 5, A-1400, Vienna, Austria*
[8]*Institute for Physics and Power Engineering (IPPE), Bondarenko Sq. 1, 249033 Obninsk, Russia*

(Received August 2, 2010 and accepted in revised form November 8, 2010)

In 1999, the IAEA has initiated a Coordinated Research Project on "Updated Codes and Methods to Reduce the Calculational Uncertainties of the LMFR Reactivity Effects." Three benchmark models representing different modifications of the BN-600 fast reactor have been sequentially established and analyzed, including a hybrid core with highly enriched uranium oxide and MOX fuel, a full MOX core with weapons-grade plutonium, and a MOX core with plutonium and minor actinides coming from spent nuclear fuel. The paper describes studies for the latter MOX core model. The benchmark results include core criticality at the beginning and end of the equilibrium fuel cycle, kinetics parameters, spatial distributions of power, and reactivity coefficients obtained by employing different computation tools and nuclear data. Sensitivity studies were performed to better understand in particular the influence of variations in different nuclear data libraries on the computed results. Transient simulations were done to investigate the consequences of employing a few different sets of power and reactivity coefficient distributions on the system behavior. The obtained results are analyzed in the paper.

KEYWORDS: reactivity coefficients, fast reactors, reactor safety, reactivity effects, kinetic parameters, uncertainties of reactivity coefficients, sensitivity to nuclear data

I. Introduction

Benchmark analyses for a BN-600 reactor core model with MOX fuel containing "Minor Actinides (MAs)" were performed in the framework of the IAEA-sponsored "Coordinated Research Project (CRP)" on "Updated Codes and Methods to Reduce the Calculational Uncertainties of the LMFR Reactivity Effects."[1–3] The general objective of the CRP was to validate, verify, and improve methodologies and computer codes used for the calculation of reactivity coefficients in fast reactors, with the aim of enhancing the utilization of plutonium and minor actinides.

The CRP activities were started in 1999 and included studies for

- a so-called hybrid BN-600-reactor-type core model, partially fuelled with highly enriched uranium and partially, about 20% of "fuel subassemblies (FSAs)," with MOX (Phases 1 to 3),
- a full-MOX core model with weapons-grade plutonium (Phase 4),
- a model of the BFS-62-3A experimental critical configuration, a mockup of the hybrid core (Phase 5) and, finally,
- a full-MOX core model with plutonium and MAs coming from spent nuclear fuel (Phase 6).

Ten organizations from nine IAEA "Technical Working Group for Fast Reactors (TWG-FR)" member states and the IAEA participated in all or in some of the CRP activities.

The hybrid and MOX BN-600 benchmark models were created on the basis of the BN-600 reactor core operating in Russia and utilizing uranium fuel. The MOX fuel of the hybrid core contains weapons-grade plutonium with a higher than 90% fraction of the fissile isotope Pu239, the hybrid core model (unlike the operating one with fertile radial and axial blankets) being surrounded by two steel shielding zones, followed by a radial reflector zone (the axial fertile blankets being retained in the hybrid core model).

The hybrid core model analyses included studies for an RZ homogeneous benchmark (Phase 1), a HEX-Z homogeneous benchmark (Phase 2), and a HEX-Z heterogeneous and burnup benchmark (Phase 3).

The studied core parameters were the effective multiplication factor, effective delayed neutron fraction and neutron lifetime, and the integral values and spatial distribu-

*Corresponding author, E-mail: Andrei.Rineiski@kit.edu

tions of reactivity coefficients relevant to reactor safety. The participants applied their own state-of-the-art basic data, computer codes, and methods to the benchmark analysis. Within the scope of these analyses, they have validated their efforts to update basic nuclear data, and to improve methodologies and computer codes for calculating safety relevant reactor physics parameters. The results for integral and local reactivity coefficient values obtained by the participants were intercompared in terms of their uncertainty resulting from different data and method approximations along with their effects on the simulated (by employing the computed parameters) core behavior under transient conditions.

In general, the diffusion approximation was found to be reasonably accurate for the considered models, while an appreciable spread in calculated parameters was observed due to the different data and computation tools employed. This spread, in particular, in spatial distributions of power and reactivity coefficients, did not influence appreciably the results of the ULOF transient simulations before sodium boiling onset due to compensation effects. However, after this onset, the mentioned spread caused a significant divergence in the characteristics of the accident progression.[1,2)]

The CRP studies were continued for a BN-600 reactor core model fully fuelled with MOX (Phase 4), containing (as before) weapons-grade plutonium. This model was designed at IPPE to reduce the sodium void effect by decreasing the fissile core height and incorporating a sodium plenum above the core, thus eliminating the upper axial fertile blanket. An internal breeding zone (IBZ) of 5.1 cm thickness was inserted at the inner core mid-plane to achieve a further reduction of the sodium void effect, an essential goal aimed in the BN-800 core design investigations. To compensate for the fissile fuel volume reduction resulting from the design changes, an extra row of FSAs was added.

Larger differences in the spatial distributions of the reactivity coefficients were observed for the full MOX core model of Phase 4. They had a larger effect on the prediction of maximal values of parameters of the UTOP and ULOF accidents in the full MOX core model in comparison with the hybrid core one. A particular source of uncertainties, especially for the sodium density coefficient, was related to the modeling of the axial sodium plenum above the fissile core. The influence of the uncertainties due to the choice of geometry approximations (RZ, HEX-Z) was found to be higher than of those due to the choice of heterogeneous/homogeneous or diffusion/transport calculation options.[3)]

Phase 5 focused on the validation of the employed tools for computing criticality values and sodium void coefficient distributions by comparison with the results of measurements made in the BFS-62 critical facility. A series of four BFS-62 critical assemblies have been designed with the aim of studying the changes in the reactor physics behavior of the BN-600 reactor from its current state to that of a hybrid core including MOX fuel. The third of these assemblies, BFS-62-3A, was considered for study in Phase 5 of the benchmark analysis. The sodium void reactivity effects have been determined for four different configurations where sodium has been removed from fuel rods within the BFS-62-3A core. The comparative analyses between experimental and calculated parameters confirmed in general the applicability of the employed codes and data libraries for computing fast reactor safety-related parameters.

The analyses were concluded by studies of Phase 6 for a core model similar to that investigated in Phase 4, but with MOX fuel containing plutonium and MAs coming from LWR spent fuel.

In the paper, the reasons for choosing the plutonium isotopic composition and MA content in the MOX fuel of Phase 6 are explained. The reactor model, provided by IPPE, is described. The obtained—by the participants—results on criticality, burnup reactivity loss, and reactivity coefficients are discussed. Outcomes of sensitivity studies on the influence of different nuclear data and of different MOX fuel compositions are described. Some results of ULOF transient analyses are shown.

II. Plutonium Isotopic Composition and MA Content in the MOX Fuel

Phases 1 to 5 addressed issues of utilization of weapons-grade plutonium in BN-600. This reactor type may also allow the efficient utilization of "transuranium (TRU)" isotopes coming from spent nuclear fuel. This issue was addressed in Phase 6 of the CRP.

Unlike weapons-grade plutonium, the plutonium isotopic composition of spent LWR fuel is characterized by a lower fraction of the Pu239 isotope, but higher fractions of other plutonium isotopes, particularly Pu240. Spent fuel may also contain an appreciable fraction of MAs, particularly of neptunium and americium isotopes. This may lead to deterioration (compared with a weapons-grade plutonium-fuelled core) of core safety characteristics.

Plutonium and MA isotopic composition in spent fuel depends on its irradiation, cooling, and reprocessing history. To establish an envelope case (with a TRU content deviating at most from weapons-grade plutonium while assuming no separation of plutonium and minor actinides during reprocessing), it was suggested to consider a 60 GWd/t reprocessed LWR uranium fuel and allowing for a fuel storage period of 50 years before reuse. For a 25% TRU content in the fuel, the MA content there would amount to more than 5% and may pose a quite challenging issue for the core transient behavior. For a smaller burnup (*e.g.*, 45 GWd/t) and/or much shorter cooling time, the MA content would be appreciably smaller. Note that in the studies performed in the past, the MA content is often[4)] limited by 5% if MAs are homogeneously mixed with other fuel components (the alternative to put MAs in special "target" subassemblies is not considered here), the limit depending upon sodium-cooled fast reactor design option (if a conventional option, established in the past, is considered).

Calculation of the heavy nuclei isotopic composition for the BN-600 benchmark was carried out at IPPE by using isotopic vectors for plutonium and MAs computed by CEA on the basis of the above-mentioned assumptions. The TRU content in MOX was adjusted as appropriate region by region. The employed refueling scheme assumed reloading

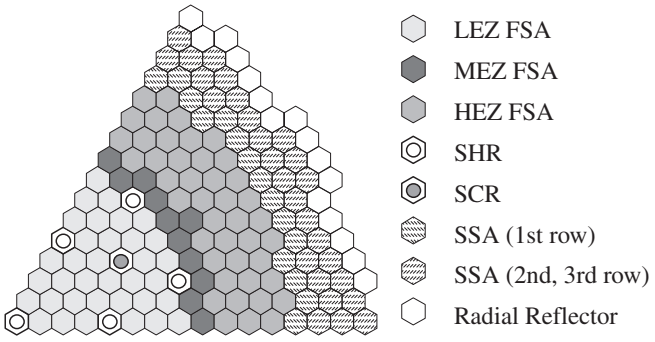

Fig. 1 Layout of the BN-600 model (60-degree sector, rotational symmetry)

of a quarter of the core every 140 effective full power days (EFPDs) *i.e.*, a four-batch reloading scheme. For the purpose of simplification, isotopic compositions for individual reloading bundles were averaged in each of three enrichment zones and then offered to the benchmark participants at a state corresponding to the beginning of an equilibrium cycle (BOC).

III. Benchmark Description

A 60-degree sector of the benchmark core layout in plane is shown in **Fig. 1**. The RZ layout of the core is given in **Fig. 2**, including heights (in cm) of reactor regions and nodes, for which spatial distributions of reactivity coefficients were computed. The core power is 1,470 MWth.

The core consists of a low-enrichment MOX inner zone (LEZ), a middle-enrichment MOX zone (MEZ), and a high-enrichment MOX zone (HEZ). In addition, there is an internal axial breeding zone (IBZ), a region with depleted uranium of 5.1 cm height at the core mid-plane in the LEZ region. Three scram control rods (SCRs) and one shim control rod (SHR) are interspersed in the LEZ region. Beyond the HEZ outer zone, there are two steel shielding zones (SSA1 and SSA2) followed by a radial reflector zone (REF). In the shim rod zone, the bottom of the absorber is parked 2.55 cm above the core mid-plane, whereas, in the scram rod zone, the absorber is parked at the bottom of the upper boron shield region.

The LEZ, MEZ, and HEZ fuel subassemblies have identical geometry with a pitch of 9.902 cm, 127 fuel pins being located with a triangular pitch of 7.95 mm inside a hexagonal wrapper. A sodium plenum followed by a boron shield is located above the core to reduce the sodium void effect. All fuel isotopes are assumed to be at a uniform temperature of 1,500 K, and all structure and coolant isotopes are at a uniform temperature of 600 K.

For this benchmark configuration, the burnup for each enrichment zone is about 2%, the TRU content in different enrichment zones varying from about 26 to 30% (from about 6 to 7% being MAs and from 20 to 23% being plutonium containing ca. 61% Pu239, 32% Pu240, a bit less than 5.5% Pu238, and small fractions of Pu241 and Pu242 isotopes). Thus, the TRU content in the fuel was about 50% higher than that for Phase 4.

Reflector	30.0	30.0	22	22	22	22	22	22	22	21
Cones	4.5	4.5	12	12	12	14	16	19	20	21
Upper Boron Shield	15.0	5.0	13	13	13	14	16 SCR	19	20	21
		5.0								
		5.0								
Cones	4.5	4.5	12	12	12	14	17	19	20	21
Sodium Plenum	23.0	8.0	11	11	11	14	17	19	20	21
		8.0								
		7.0								
Plugs	5.3	5.3	10	10	10	14	17	19	20	21
Core	41.15	8.23	1 LEZ	2 MEZ	3 HEZ	14 SHR	17	19 SSA1	20 SSA2, 3	21 Radial Reflector
		8.23								
		8.23								
		8.23								
		8.23								
IBZ	5.1	5.1	23 IBZ	2	3	15	18	19	20	21
Core	41.15	8.23	1 LEZ	2 MEZ	3 HEZ	15	18	19 SSA1	20 SSA2, 3	21 Radial Reflector
		8.23								
		8.23								
		8.23								
		8.23								
A. Blanket 1	5.5	5.5	7	8	9	15	18	19	20	21
Axial Blanket 2	29.7	9.7	4	5	6	15	18	19	20	21
		10.0								
		10.0								
Reflector	30.0	30.0	22	22	22	22	22	22	22	21

Fig. 2 RZ arrangement of the compositions for the BN-600 core model

The CRP participants were asked to compute the following parameters: criticality (k_{eff}), effective delayed neutron fraction (β_{eff}), fuel Doppler coefficient, sodium density coefficient, fuel density coefficient, radial expansion coefficient, and axial expansion coefficient. The participants were also asked to perform burnup calculations for one cycle (140 EFPDs) as a single step (*i.e.*, without recomputing the neutron flux and neutron cross sections during the cycle) assuming that the control rods were at the fixed insertion as defined in Fig. 2. The core power was normalized by assuming all power being deposited at the point of fission, energy per fission of 200 MeV, and zero energy per capture for all nuclides. At the end of the cycle (EOC), the isotopic nuclear densities for reactor regions, criticality, and, optionally, the parameters mentioned above were requested.

For all reactivity coefficients, the integral values were to be obtained by direct calculations. For all reactivity coefficients, except those for radial and axial expansion, spatial distributions were also to be computed by employing first-order perturbation theory (FOPT). The density and expansion coefficients were (similar to Phases 1 to 4) defined as reactivity effects due to variations in the corresponding material densities (by 1%) and dimensions (height, radius), respectively, normalized by relative variations in the corresponding (density, dimension) parameters. Fuel temperature variations from $T = 1{,}500$ K to $T = 2{,}100$ K and steel temperature variations from $T = 600$ K to $T = 900$ K were considered for computing the Doppler coefficients while assuming linear variations of criticality *vs.* $\ln(T)$.

Table 1 Reactor physics parameters of BN-600 model with MOX containing MAs at BOC computed by CEA&SERCO, KIT, and IPPE

	CEA&SERCO, JEF-2.2/JEFF3.1 1968→33 gr. (Phase 4 JEF-2.2)	KIT, JEFF-3.0, 30→21gr./560→21 gr. (Phase 4)	IPPE, ABBN-93 26→18gr./FOPT (Phase 4)
k_{eff}	0.98829/1.00386	0.99069	0.99517
Fuel Doppler, pcm	−401/−408 (−789/−794)	−351/−379 (−698/−766)	−337/−341 (−684)
Steel Doppler, pcm	−80 (−124)	−61	
Sodium density, pcm	−1,680/−1,489 (−199)	−1,124	/−1,140 (139)
Fuel density, pcm	44,560 (38,820)	37,807	/37,000 (37,860)
Steel density, pcm	−3,910	−3,496	/−3,200 (−126)
Radial expansion, pcm	−5,198	−5,317	
Axial expansion, pcm	−1,404	−1,485	
β_{eff}, pcm	307 (350)	298	299 (344)
Neutron lifetime, μs	0.309 (0.436)	0.296	

Table 2 Reactor physics parameters of BN-600 model with MOX containing MAs at BOC computed at IGCAR, JAEA, and KAERI

	IGCAR, XSET 98, 26 gr. (Phase 4)	JAEA, JENDL-3.2, 70→18gr. (Phase 4)	KAERI, JEFF3.1 150→25gr./ JEF-2.2 80→9 gr. (Phase 4)
k_{eff}	1.00238	0.99194	1.00658/0.99022
Fuel Doppler, pcm	−371 (−732)	−371 (−770)	−424/−438 (/888)
Steel Doppler, pcm		−63 (−100)	−65/−71 (−101)
Sodium density, pcm	−1,392 (−15)	−1,571 (84)	−1,133/−1,324 (223)
Fuel density, pcm	37,057 (37,670)	37,698 (39,080)	37,305/37,820 (37,220)
Steel density, pcm	−3,368 (−185)	−3,673 (−159)	−2,907/−2,854 (−41)
Radial expansion, pcm		−5,287	−5,251/5,351
Axial expansion, pcm		−1,489	−1,428/1,455
β_{eff}, pcm	297 (346)	299 (336)	302 (342)
Neutron lifetime, μs	0.318 (0.451)	0.312 (0.448)	0.309 (0.426)

All the parameters were to be calculated by employing homogeneous representations of the material regions and the neutron diffusion theory in 3D HEX-Z geometry.

IV. Benchmark Results at BOC

The results on criticality, integral reactivity coefficients and other parameters obtained by benchmark participants at BOC are shown in **Tables 1** and **2**, where "Fuel Doppler," "Steel Doppler," "Sodium density," "Fuel density," "Steel density," "Radial expansion" and "Axial expansion" stay for the respective reactivity coefficients.

The first column of Table 1 shows the parameters delivered as a combined contribution of CEA&SERCO by employing two fine-group (1968 groups) cross section libraries: (1) based on JEF-2.2[5] (for all benchmark parameters) and (2) on JEFF-3.1[6] (for a restricted set of parameters). For the core calculations, the fine-group effective (*i.e.*, after taking self-shielding effects into account) cross sections were condensed to 33 groups by using fine-group spectra calculated for homogeneous cell models. For example, the k_{eff} values—obtained with the JEF-2.2 and JEFF-3.1 data—are 0.98829 and 1.00386, respectively. Some reactivity coefficients are provided for both Phase 4 and Phase 6 benchmark models, the values in brackets showing the Phase 4 results. For example, the Fuel Doppler constant for Phase 6 (−401 and −408 pcm for the JEF-2.2 and JEFF-3.1 data options, respectively) is about 50% lower than that for Phase 4 (−789 and −794 pcm for the JEF-2.2 and JEFF-3.1 data options, respectively). For the fuel density, steel density, radial expansion, and axial expansion coefficients and for the kinetics parameters, only the results obtained with JEF-2.2 are given. The sodium density coefficient increased appreciably by a magnitude compared with Phase 4 (to −1,680 and −1,489 pcm for the JEF-2.2 and JEFF-3.1 data options, respectively, compared with −199 pcm for the JEF-2.2 option in Phase 4). That means a much higher positive coolant void effect. The kinetics parameters are smaller than those for Phase 4. Thus, the reactor physics parameters for this core are less favorable (compared with those for the core studied in Phase 4) with regards to reactor safety. This is in line with the results of the other benchmark participants discussed in the following. CEA also performed studies to analyze energy and nuclide contributions to computed parameters, some results of which are discussed later.

The KIT results are given in the second column of Table 1. They were obtained by employing two JEFF-3.0-based multigroup libraries: a 30-group library and a 560-group one. In both cases, the effective cross sections were condensed to 21 groups with cell-wise spectra, the 21-group cross sections being employed for the core analyses. Initially, a full set of benchmark parameters was obtained with the 30-group library, but the fuel Doppler constant appeared to be low by a magnitude compared with those of some participants. One of the possible reasons was assumed to be the insufficient number of energy groups in the employed data library. Therefore, the fuel Doppler calculations were performed also with the 560-group data condensed with cell-wise spectra to 21-group cross sections. That resulted in a higher absolute value of the constant by ca. 30 pcm or by about 10%. Calculations with the fine-group library were then performed for the Phase 4 model, leading to the same relative (but higher absolute) variation from −698 to −766 pcm (due to the use of the 560-group library instead of the 30-group one) as shown in Table 1.

Column three of Table 1 shows the IPPE results obtained with a 26-group library, ABBN-93. The 26-group effective cross sections were condensed to 18 groups and employed for the core calculations. Only the results based on FOPT are available (including the integral reactivity coefficients), except for k_{eff} and fuel Doppler constant (integral parameters, computed directly and by FOPT, −337 and −341 pcm, respectively). The IPPE results are in line with those of the other participants as regards ratios of the fuel Doppler constants for Phase 4 and Phase 6. All density coefficients in Table 1 for Phase 4 (unlike those shown for Phase 4) are obtained by employing the FOPT option.

The IGCAR results (column one of Table 2) were obtained with 26-group effective cross sections generated from a library of the ABBN type, XSET 98. The results for Phase 4 deviate slightly from those given in Ref. 3) due to modifications in the employed calculation procedure. The leakage and nonleakage components of the sodium density coefficient were evaluated by IGCAR as 2,664 and −4,056 pcm, respectively, for Phase 6, while as 2,989 and −2,974 pcm, respectively, for Phase 4. One may observe relatively minor variations in the leakage component as the core geometry is the same, but strong variations in the nonleakage component due to the higher content of Pu240 and MAs.

Column two of Table 2 shows the JAEA results. JAEA employed the same computation procedure for all CRP stages by employing a basic 70-group library based on JENDL-3.2[7] and condensing the effective cross sections to 18 energy groups with cell-wise spectra. Variations in the computed parameters between Phase 4 and Phase 6 are similar to the average (of all participants) ones. As for earlier phases, JAEA performed a broad scope of sensitivity studies described in the following.

The KAERI results are given in the last column of Table 2. Results for two cross section generation options are shown: (1) a 150-group library based on JEFF-3.1, the effective 150-group cross sections being condensed to 25 groups, and (2) an 80-group library based on JEF-2.2 and condensing the data to 9 groups (the latter option was used also for Phase 4). The fine group (150-group and 80-group) spectra used for condensation were computed for a 2D RZ core model by employing a neutron transport model.

The highest criticality values were obtained with JEFF-3.1 data, the lowest ones with JEF-2.2. The effect of using JEFF-3.1 instead of JEF-2.2 is predicted similarly by CEA&SERCO and KAERI: by a value between 1,550 and 1,850 pcm (the criticality values being higher in the KAERI case). For Phase 4, the effect of using JEFF-3.1 instead of JEF-2.2 was much smaller, about 200 pcm (a result of CEA). This may be seen as an indication of larger uncertainties in reactor physics parameters while employing fuels with a higher content of MAs.

The lowest (by a magnitude) fuel Doppler coefficients were obtained by KIT (in the case of using the 30-group library) and IPPE. This may be related to a relatively low number of energy groups in the basic data library, this conclusion being confirmed in the KIT case (as explained above). The highest coefficient was computed by KAERI, similar to Phase 4, probably reflecting specific features of the employed computation procedure.

The lowest (by a magnitude) sodium density coefficients were obtained by KIT, IPPE, and KAERI (with JEFF-3.1), the highest values being provided by CEA&SERCO (JEF-2.2) and JAEA. One may partly associate this observation with newly evaluated Na cross sections (as concerns the contributions of elastic and inelastic scattering to the total neutron scattering) available from JEFF-3.0 and JEFF-3.1. The use of JEFF-3.1 data—as compared with JEF-2.2—yields an absolute value of the density coefficient that is lower by ca. 200 pcm.

The highest values for the fuel density and (by a magnitude) for the steel density coefficients were obtained by CEA&SERCO, exceeding the results of the other participants by about 10% or more. Further analyses are needed to understand whether the use of a much finer (as compared with those of other participants) basic data library is the reason for the observed deviations.

The expansion coefficients do not show a large spread prompting a conclusion that their uncertainties due to nuclear data and computation options are not too high, especially taking into account existing uncertainties in the modeling of the core thermal expansion during the transient. The kinetics parameters are in reasonable agreement.

V. Burnup Modeling

The burnup analyses and reactivity coefficients for EOC were delivered by CEA&SERCO, KIT, JAEA, and KAERI by employing the JEF-2.2-based data, 30-group JEFF-3.0-based data, JENDL-3.2-based data, and JEFF-3.1-based data, respectively. The burnup reactivity loss values after 140 EFPDs are given in **Table 3**.

The average (of the participants) variations of the nuclear density of the main fuel isotopes in the LEZ region and the ratios (of the results of the participants) to the average values are given in **Table 4**.

The results of the participants are in general agreement. Relatively strong deviations of the ratios from unity for

Table 3 Reactivity loss after 140 EFPDs

	CEA&SERCO	KIT	JAEA
Reactivity loss, pcm	456	594	541

Pu240 are partly related to a very small absolute variation of the Pu240 nuclear density. The ratios for Am242m (anti-)correlate to the reactivity loss. One should note that different branching ratios for Am241 capture cross section were employed by different participants. CEA&SERCO and JAEA employed a value of 0.85 (that means probabilities of 85 and 15% to get Am242 and Am242m nuclei, respectively, after a neutron capture by an Am241 nucleus), while KIT employed energy-dependent probabilities from the JEFF-3.1 activation file, effectively yielding a value near 0.90 for the considered composition. It was observed in earlier analyses that a higher branching ratio leads to a higher reactivity loss for MA-bearing fuels. This observation was supported by analyses performed by JAEA for Phase 6, in which a simplified burnup chain and a lower branching ratio of 0.8 were employed, resulting in a reactivity loss of 387 pcm (instead of 541 pcm, see Table 3).

Deviations between the reactivity coefficients provided by CEA, KIT, JAEA, and KAERI at EOC are similar to those at BOC.

The transport and heterogeneity effects were not addressed in Phase 6. They were evaluated before, particularly for Phase 4. The results of Phase 4 have shown that the criticality values provided by transport theory were higher by a value near 600 pcm (a similar value was obtained by CEA for Phase 6), while the integral sodium density coefficient (opposite to the void one) was lower by a value near 200 pcm if the transport theory was employed.

Heterogeneity treatment resulted in higher criticalities (by about 300 pcm) and in variations of the sodium coefficient, which were similar in magnitude, but opposite in sign to those due to the use of the transport approach instead of the diffusion theory. The effect of the application of transport and heterogeneous calculation models (instead of diffusion homogeneous ones) with respect to the Doppler coefficients was found to be small in Phase 4 studies.

VI. Analyses of Energy and Nuclide Contributions

CEA performed a series of analyses to investigate energy and nuclide contributions to the observed variations (from Phase 4 to Phase 6) in computed parameters. The direct and adjoint flux spectra for the MOX fuel options considered in the 2 benchmarks are provided in **Figs. 3** and **4**.

The energy scale in Figs. 3 and 4 is given by group numbers of the 33-group structure, groups 20, 10, and 5 being bounded by the following energies (keV): ca. 0.749 and 1.23, 111 and 183, 1350 and 2230, respectively. One may conclude that the neutron flux spectra are slightly "harder," while the adjoint ones are appreciably "harder" for Phase 6. The latter effect is a consequence of the higher threshold fission due to the higher content of Pu240 and the presence of MAs in the fuel. The relatively lower importance of neutrons at lower energies for the MA-bearing fuel leads to a higher (lower by a magnitude) fuel Doppler constant and to a lower (increased by a magnitude) sodium density coefficient.

In **Fig. 5**, one may see that contributions to the fuel Doppler constant come mainly from energies near 1 keV (near group 20); therefore, the absolute value of this parameter is smaller in Phase 6. The sharp variations of the curve—shown in Fig. 5—result from the two compensating effects: an increase in neutron absorption by fertile isotopes (main contributors to the Doppler effect) at low energies and a decrease in the neutron flux. The first factor determines the curve behavior above 1 keV, and the second one dominates at lower energies. The steep variations of the curve near 1 keV may also be the reason for underestimating the Doppler constant if the basic library with a relatively low number (*e.g.*, 30) of energy groups is employed, as the spectra used for computing the cross sections employed in core calculations may not be accurate enough to take the observed effects into account. More analyses are needed to confirm this suspicion.

Table 4 Nuclear density variations in the LEZ region after 140 EFPDs

	Nuclear density at BOC, at/barn/cm	Average variation after 140 EFPDs, at/barn/cm	Ratio to the average by CEA	Ratio to the average by KIT	Ratio to the average by JAEA	Ratio to the average by KAERI
U238	5.823E−03	−0.000122	0.98	1.02	1.00	1.00
Np237	1.321E−04	−0.000014	0.97	0.99	1.05	1.00
Pu238	8.871E−05	0.000013	1.05	1.00	1.00	0.95
Pu239	9.959E−04	−0.000039	1.00	1.02	1.03	0.95
Pu240	5.179E−04	−0.000001	1.68	0.78	2.13	−0.59
Pu241	2.341E−05	0.000011	1.06	0.94	1.12	0.88
Pu242	6.243E−06	0.000005	0.99	1.09	0.97	0.95
Am241	2.827E−04	−0.000035	1.01	1.05	0.96	0.98
Am242m	4.353E−06	0.000003	1.08	0.49	0.97	1.46
Am243	4.118E−05	−0.000004	1.01	1.06	0.95	0.98
Cm242	1.494E−05	0.000008	1.06	1.24	0.87	0.83

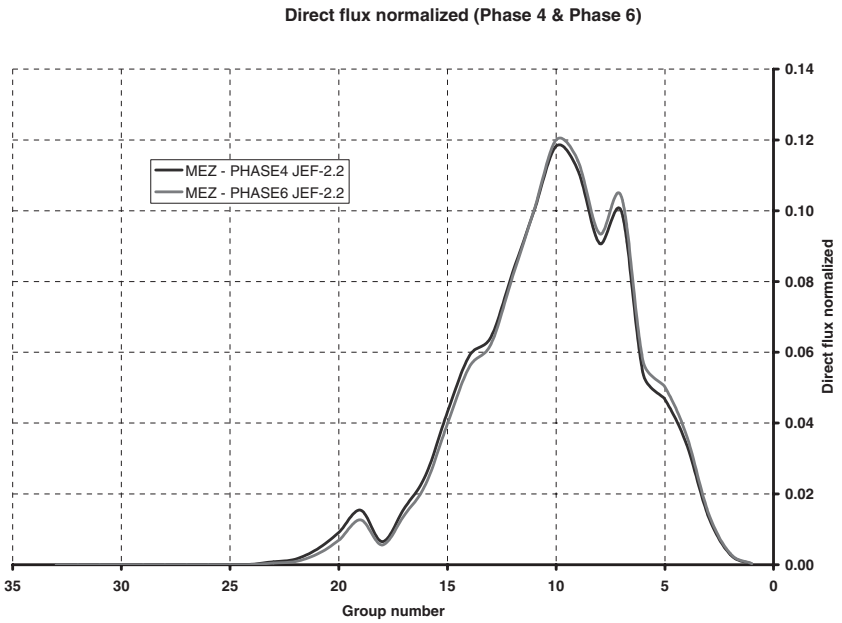

Fig. 3 Neutron flux spectra in the MEZ region for the two MOX fuel options

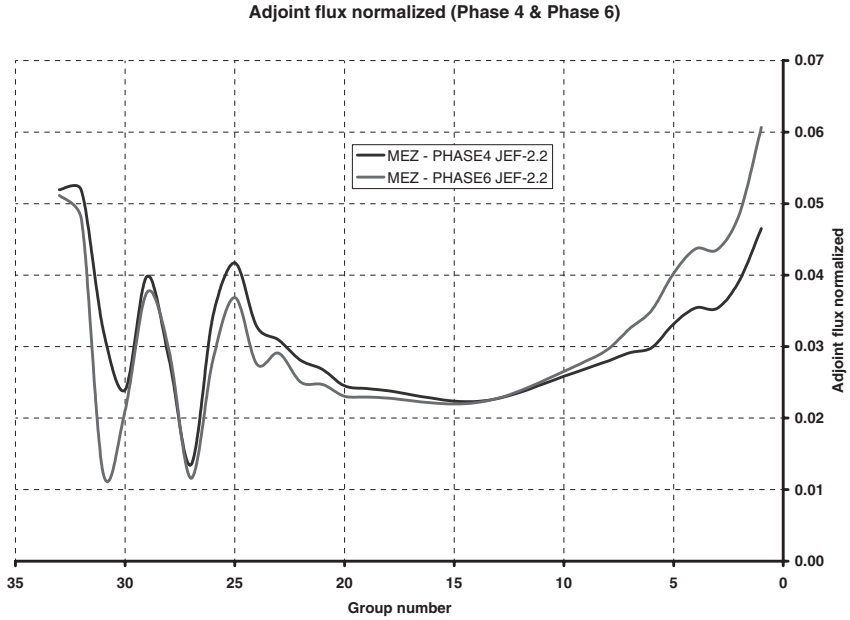

Fig. 4 Adjoint flux spectra in the MEZ region for the two MOX fuel options

The nuclide contributions to the core reactivity for the two considered MOX fuel options can be analyzed by considering the so-called reactivity equivalence coefficients (see **Table 5**), assuming that the coefficient for U238 is zero and that Pu239 is one. A negative value indicates that the nuclide is a stronger—than U238—net absorber, while a higher—than one—value indicates that the nuclide is a stronger—than Pu239—net neutron generator. An intermediate value (*e.g.*, 0.5) indicates that with respect to the contribution to the neutron balance, the nuclide is an intermediate between U238 and Pu239 (*e.g.*, the two nuclei are equivalent to a combination of U238 and Pu239 nuclei).

Data of Table 5 confirm that the relative importance of high-energy neutrons increases after Pu240 and MAs are added to the fuel. For example, the observed augmentation of the coefficient for Pu240 may be associated with an increased contribution of the Pu240 threshold fission rate to the total fission one.

Increase in the sodium density coefficient between Phase 4 and Phase 6 was found to be mainly due to increased contents of Pu240, Np237, and Am241 in the fuel that was only partially compensated by a reduced content of U238 (see **Table 6** obtained with JEFF-3.1 data at BOC). Table 6 includes also a contribution of the fission products (FPs) of Pu239.

The total effect—of the variation of the fuel composition on the variation of the sodium density coefficient—as predicted by FOPT is not exactly the same (as one may obtain

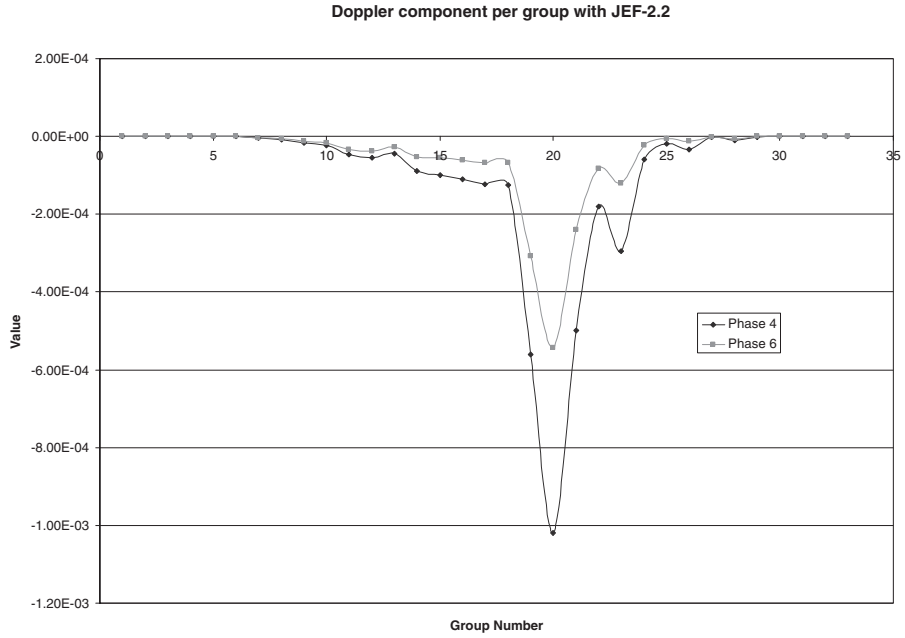

Fig. 5 Energy contributions to the fuel Doppler constant

Table 5 Equivalence coefficients computed with JEF-2.2 data at BOC

Nuclide	Phase 4	Phase 6
Np237	−0.244	−0.196
Pu238	0.599	0.625
Pu240	0.126	0.155
Pu241	1.462	1.411
Pu242	0.089	0.109
Am241	−0.308	−0.258
Am243	−0.297	−0.251
Am242m	2.150	2.071

Table 6 Nuclide contributions to variations of the sodium density effect from Phase 4 to Phase 6

Nuclide	Contribution
U238	−1.87E−03
Pu238	2.28E−04
Pu239	1.39E−03
Pu240	5.49E−03
Pu241	−6.26E−04
Np237	3.53E−03
Am241	6.77E−03
Am242m	−2.04E−04
Am243	8.42E−04
Solid FPs of Pu239	−1.94E−04
TOTAL	1.56E−02
MAs	1.14E−02
Pu	6.32E−03
U	−1.92E−03

by employing the results of Table 1), but the accuracy is sufficient to evaluate the effect and contributions of particular nuclides.

The performed analyses underline the importance of the presence of Am241, the main MA component, in the fuel with respect to the degradation of the reactivity coefficients.

VII. Sensitivity Studies on Effects of Using JENDL-3.2 and JEFF-3.1 Data

JAEA studied the effects of employing JEFF-3.1 data instead of JENDL-3.2 ones. The 18-group average cross sections were computed on the basis of the corresponding libraries at KAERI and JAEA. Since KAERI provided only the total scattering data, JAEA subdivided them into the elastic and inelastic parts by using the ratio of the JENDL-3.2 library (this approach is certainly an approximation, in particular taking into account that a new ratio for sodium was adopted for JEFF-3.1). The average cosine values for JEFF-3.1 were neither available to JAEA and, therefore, assumed to be the same as those for JENDL-3.2.

Some results of the sensitivity analyses, showing contributions from particular nuclides and nuclear reactions, are given in **Figs. 6**, **7**, and **8** (criticality, sodium density coefficient, reactivity loss after 140 EFPDs, *etc.*).

The differences between the results obtained with the libraries are affected by a large cancellation of contributions from many nuclides and reactions, especially U238 inelastic (JAEA did not get the exact one of JEFF-3.1 from KAERI as mentioned above), Pu239 FP capture (there are many different ways to generate the lumped FP cross sections), Pu239 fission (due to its large sensitivity), Am241 capture (need to be investigated), Pu238 fission, Pu240 nu-bar value, oxygen capture, nickel capture, *etc.*

The comparisons between the library effects ((JEFF-3.1 − JENDL-3.2)/JENDL-3.2 ∗ 100%) obtained by direct calculations and by employing the FOPT approach in sensitivity studies are provided in **Table 7**.

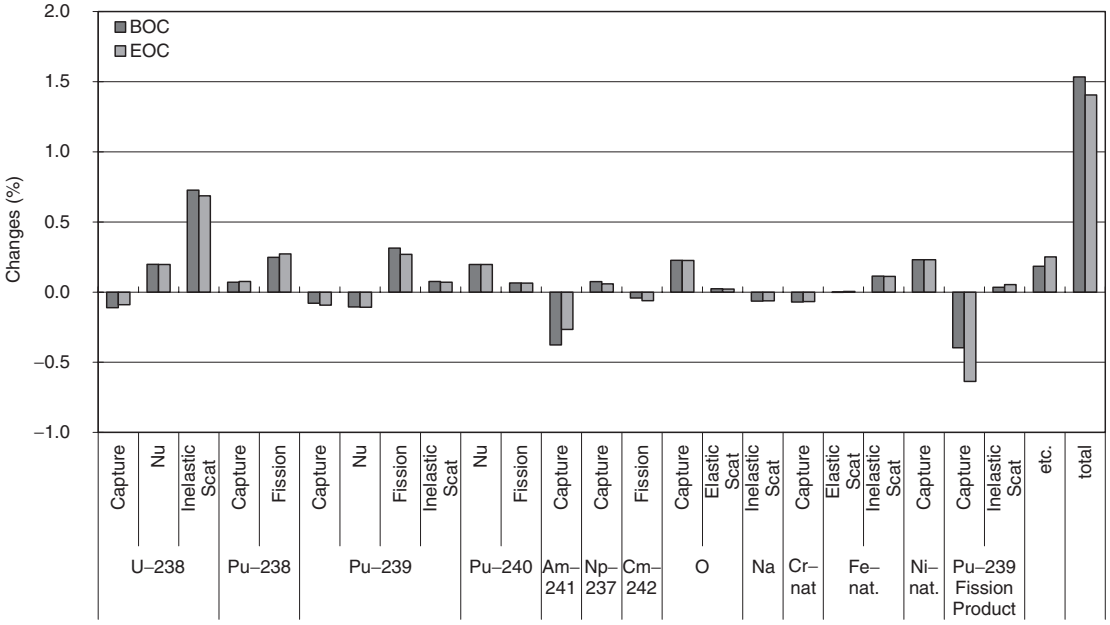

Fig. 6 Contributions to variations in criticality (JEFF-3.1 instead of JENDL-3.2)

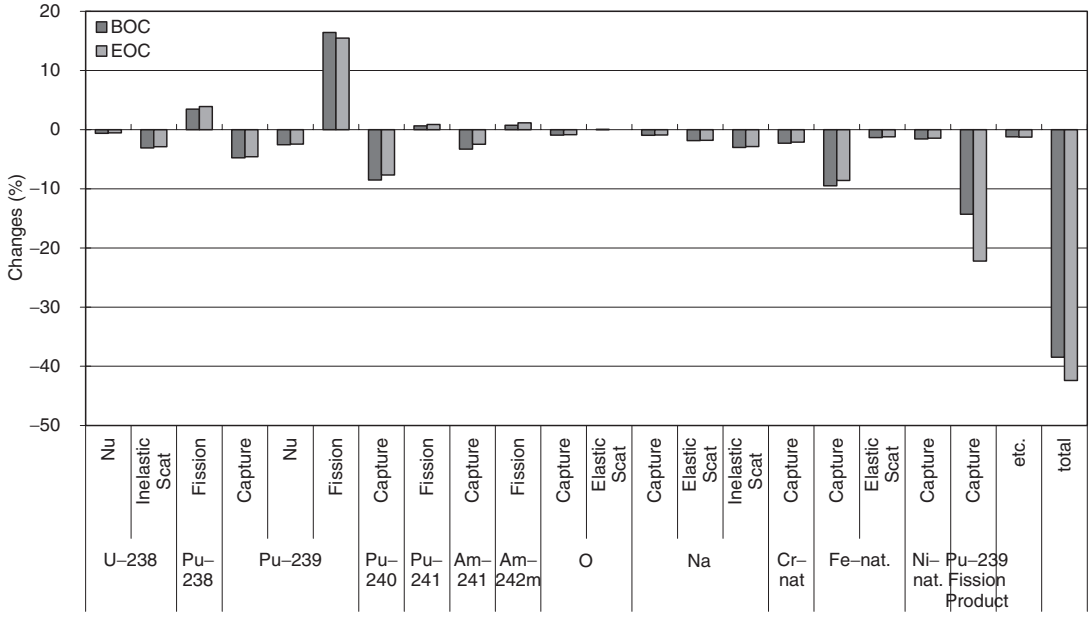

Fig. 7 Contributions to variations in sodium density coefficient (JEFF-3.1 instead of JENDL-3.2)

One may conclude that the sensitivity approach is reasonably accurate and may help to identify the main contributions from particular nuclides and nuclear reactions as concerns the criticality and reactivity coefficients. For the burnup results, this approach is less accurate in the considered case because only variations in principal cross sections were taken into account while variations in other parameters (burnup chains, branching ratios, and decay constants) were neglected. For example, the burnup reactivity loss variation due to the use of an alternative to JENDL-3.2 data is negative (the reactivity loss is lower by 37.5%) according to the direct calculations, but positive according to sensitivity ones (this parameter is higher by 23.5%).

VIII. Transient Simulation

ULOF transient simulations were performed at IPPE by employing the preliminary results of IPPE, JAEA, and KAERI, so that the fuel Doppler coefficient varied from the lowest (IPPE) to the highest (KAERI) value. Note that for Phase 4, parameters computed by seven participants were considered.

A simplified simulation approach was employed, in which no phase transition (*i.e.*, sodium boiling or structure melting) was modeled.[9] A limited time interval at the beginning of the transient was considered. Similar to Phase 4, a sodium flow rate of 30% (compared with nominal conditions) was

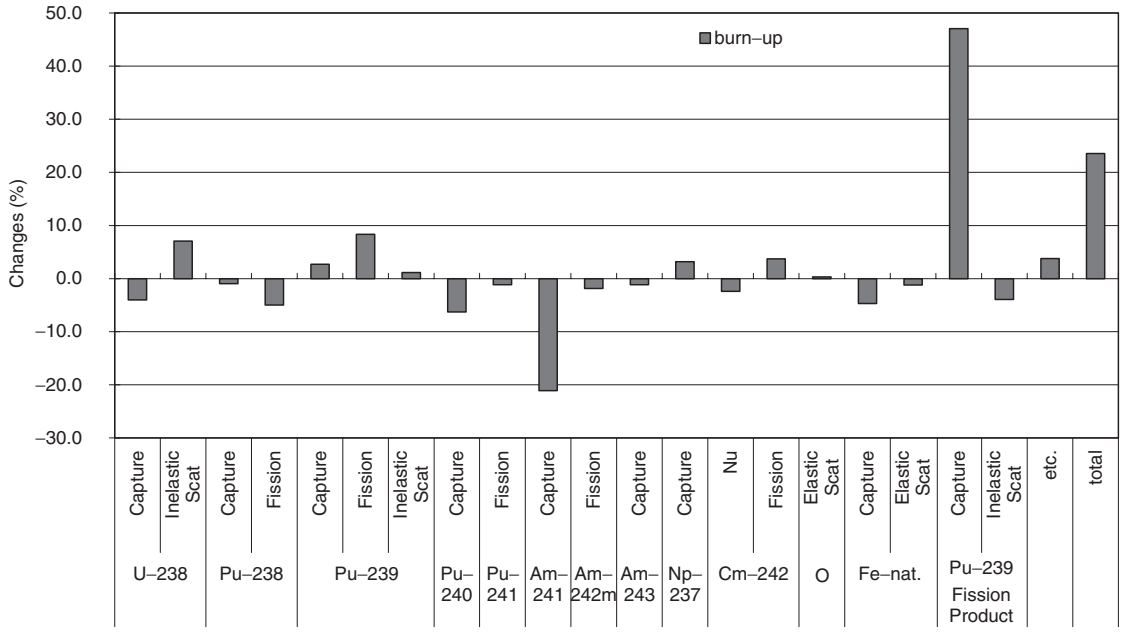

Fig. 8 Contributions to variations in reactivity loss after 140 EFPDs (JEFF-3.1 instead of JENDL-3.2)

Table 7 Sensitivity and direct calculation results on parameter variations (%) due to the use of JEFF-3.1 instead of JENDL-3.2

	Sensitivity	Direct
Criticality, BOC	1.53	1.48
Criticality, EOC	1.41	1.68
Sodium density coefficient, BOC	−38.5	−27.9
Sodium density coefficient, EOC	−42.4	−34.1
Burnup reactivity loss	23.5	−37.5
Atomic number density of LEZ region at EOC		
Pu-239	−0.2	0.3
Pu-241	−4.0	−7.2
Am-241	−1.2	−0.3
Np-237	0.0	0.7
Cm-242	6.2	−1.4
Cm-245	1.9	2.2

Table 8 ULOF transient results for BN-600, MOX fuel with MAs of Phase 6, BOC

Time (s)	0	20	40	100
Net reactivity, pcm	0	−325 (±30)	−150 (±20)	−40 (±5)
Sodium outlet temperature, °C	500	710 (±2)	720 (±5)	730 (±12)
Power (relative to $t = 0$)	1	0.75 (±0.01)	0.68 (±0.02)	0.66 (±0.03)

Table 9 ULOF transient results for BN-600, MOX fuel of Phase 4, BOC

Time (s)	0	20	40	100
Net reactivity, pcm	0	−500 (±100)	−210 (±50)	−60 (±10)
Sodium outlet temperature, °C	500	780 (±20)	770 (±20)	760 (±20)
Power (relative to $t = 0$), IPPE	1	0.65	0.63	0.62
Maximal fuel temperature, IPPE, °C	2,300	1,800	1,750	1,700

assumed to be reached after about 12 s and then remained constant. Unlike Phase 4, the radial expansion reactivity effect was assumed to be negligible. A limited set of transient simulation results was provided by IPPE, mainly as plots; therefore, a limited number of parameters is given for Phase 6 in **Table 8** and compared with those of Phase 4 (see **Table 9**).

For Phase 6, the use of the IPPE parameters led to lower sodium outlet temperatures than those of KAERI and JAEA, so a certain spread in computed parameters was observed. Therefore, the results of Table 8 show approximate mean values and the range in which the parameters vary.

The reactivity variations in Phase 4 were mainly affected by positive fuel Doppler and negative radial expansion contributions. The positive sodium density effects and negative axial expansion effects were much smaller and partly compensated each other.

Phase 6 results show a certain similarity, but they are different due to the mentioned assumption on the radial expansion effect, a lower (by a magnitude) fuel Doppler constant and higher (by a magnitude) sodium density coefficients. As earlier, one may observe that deviations in the reactivity coefficients may not lead to substantial variations in transient results at the beginning of the initial phase of the ULOF transient. More studies are needed to investigate the effect of uncertainties in reactor physics parameters on transient results for extended-in-time transient ULOF simulations and other than ULOF cases.

With the limited amount of results available, no definite conclusion on the reactor safety can be made. On the other hand, the available results do not give any particular reason that would prevent the utilization of weapons-grade plutonium or TRUs from LWR spent fuel in a BN-600-type reactor.

IX. Conclusions

A BN-600 core model with MOX fuel containing a substantial amount of minor actinides (MAs), more than 5% in the fresh fuel, was investigated in Phase 6 studies of the IAEA Coordinated Research Project on "Updated Codes and Methods to Reduce the Calculational Uncertainties of the LMFR Reactivity Effects." To establish an envelope case (with a TRU content deviating at most from weapons-grade plutonium while assuming no separation of plutonium and minor actinides during reprocessing), it was suggested to consider a 60 GWd/t reprocessed LWR uranium fuel and allowing for a fuel storage period of 50 years before reuse. Thus, the problem of utilizing TRUs coming from spent LWR nuclear fuel in BN-600-type reactors was addressed.

The computation model for a beginning of an equilibrium fuel cycle was established at IPPE by employing the TRU isotopic composition evaluated at CEA. Reactor physics parameters relevant for safety analyses were computed by institutions representing several IAEA member states while employing their up-to-date computation tools and data libraries.

The obtained values for criticality, reactivity coefficients, burnup reactivity loss, and variations in the fuel composition due to burnup are in qualitative agreement. The parameters computed by different benchmark participants show the same trends with respect to those computed for a previous benchmark phase for a similar reactor model, but with MOX fuel containing weapons-grade plutonium. In particular, the absolute value of the fuel Doppler constant is lower by about 50% or more, the sodium density coefficient increased appreciably (by a magnitude), and the effective delayed neutron fraction and neutron lifetime became smaller. This is in line with the trend observed worldwide in transmutation studies: the safety parameters deteriorate if MAs are put in the fuel.

A higher MA content leads to higher deviations in criticality due to the use of JEFF-3.1 instead of JEF-2.2 data as compared with Phase 4. A quite large relative spread in the obtained values for the fuel Doppler constant was observed initially, but later reduced after recalculations. These observations indicate a potentially higher uncertainty of computed reactor parameters in the case of using fuel with MAs instead of MOX with weapons-grade plutonium.

Sensitivity studies performed by CEA and JAEA help to understand the origin of deviations between the results of Phase 4 and Phase 6, nuclide and energy contributions to the reactivity effects, and influence of different data evaluations on the computed parameters. The benchmark has shown that the use of a relatively small (about 30) number of energy groups may lead to an underestimation of the absolute value of the fuel Doppler coefficient by a value of the order of 10%.

A limited set of transient results was provided by IPPE for the beginning of the ULOF initiation phase, while employing a few different sets of reactor physics parameters. The results confirm an earlier observation on a substantial effect of compensations of deviations between the parameters with respect to their influence on transient progression at the considered transient phase (it was shown earlier that this compensation no longer takes place at later transient phases).

The available results of the study do not indicate any reason that would prevent the utilization of weapons-grade Pu or TRUs from LWR spent fuel in a BN-600-type reactor. The ULOF transient is only a part of the safety dossier but it may be the transient, the most sensitive to the reactivity effects, particularly in the case of employing MA-bearing fuels.

One may also note the possible flexibility with which a BN-600-type core can utilize different kinds of TRU compositions, particularly those recycled from LWR spent fuels.

References

1) Y. I. Kim *et al.*, "BN-600 hybrid core benchmark analyses," *Proc. PHYSOR 2002 Int. Conf.*, Seoul, Korea, Oct. 7–10, 2002 (2002), [CD-ROM].
2) *BN-600 Hybrid Core Benchmark Analyses*, IAEA-TECDOC-1623, IAEA (2010).
3) Y. I. Kim *et al.*, "BN-600 full MOX core benchmark analysis," *Proc. PHYSOR 2004 Int. Conf.*, Chicago, Illinois, USA, Apr. 25–29, 2004 (2004), [CD-ROM].
4) K. Fujimura *et al.*, "Minor actinides-loaded FBR core concept suitable for the introductory period in Japan," *J. Power Energy Syst.*, **3**[1], 136–145 (2009).
5) C. Nordborg, M. Salvatores, "Status of the JEF evaluated data library," *Proc. Int. Conf. on Nuclear Data for Science and Technology*, Gatlinburg, Tennessee, USA, May 9–13, 1994, Vol. 2, 680 (1994).
6) Nuclear Energy Agency, *The JEFF-3.1 Nuclear Data Library*, JEFF Report 21, NEA No. 6190, OECD/NEA (2006).
7) Nuclear Energy Agency, *The JEFF-3.0 Nuclear Data Library*, JEFF Report 19, NEA No. 3711, OECD/NEA (2005).
8) T. Nakagawa *et al.*, "Japanese evaluated nuclear data library version 3 revision-2: JENDL-3.2," *J. Nucl. Sci. Technol.*, **32**, 1259 (1995).
9) A. Danilytchev, D. Elistratov, V. Stogov, *Reactivity Coefficients and Simplified Approach to Accident Process Modeling (Phase 4)*, IAEA-RC-803.4, TWG-FR/113 (2003).